SPICE Model of SPAD Transient Intrinsic Response Validated using Mixed-Mode TCAD Simulations

Tom Klauner
ICTEAM,
Université catholique de Louvain
Louvain-la-Neuve, Belgium

Iman Sabri Alirezaei
TE Connectivity
Peter-Behrens-Str 15, 12459 Berlin, Germany
iman.sabri@te.com

Nicolas Roisin
ICTEAM,
Université catholique de Louvain
Louvain-la-Neuve, Belgium
nicolas.roisin@uclouvain.be

Nicolas André
ICTEAM,
Université catholique de Louvain
Louvain-la-Neuve, Belgium
nicolas.andre@uclouvain.be

Denis Flandre
ICTEAM,
Université catholique de Louvain
Louvain-la-Neuve, Belgium
denis.flandre@uclouvain.be

***Abstract*—This work presents a SPICE compact macro-model for the transient intrinsic response of a Single-Photon Avalanche Diode (SPAD) pixel to a light pulse. The physical phenomena and related parameters are evaluated by performing mixed-mode TCAD simulations. The model is composed of three equivalent diode sub-circuits with their respective junction capacitance adapted to describe the successive mechanisms conditioning the intrinsic transient photo-response of the SPAD. After considering a light pulse, the SPICE model fairly reproduces the TCAD fast current pulse with a peak of about 2mA and a time constant of about 3ps, followed by a diffusion current response with a time constant of 35ps. It results in a self-sustaining current of about 8µA with a diode cathode voltage of 6.3V. Finally, it models the slow recharge through the quenching resistor with a time constant of 264ns. The proposed model facilitates the design of a compatible read-out circuit, e.g., with active recharge, by accurately reproducing physical current and voltage responses.**

***Index Terms*—single photon avalanche diode (SPAD), TCAD, SPICE, transient**

I. Introduction

Single Photon Avalanche Diodes (SPADs) have become of great interest in numerous applications, including Light Detection and Ranging (LiDAR), Positron Emission Tomography (PET) scanners, and Time-of-Flight (TOF) spectroscopy [1], due to their ability to detect very low light levels.

A front-end circuit is required to read out the signal and reset the avalanche diode after each detection. To design and optimize such a system using SPICE circuit simulations, an equivalent compact model of the diode is required. Various ones have already been proposed to describe the SPAD behaviour [2] [3] [4]. Most are empirical and rely on measurements to extract their parameters, which are affected by parasitic elements and the pulse shaping of the instrumentation circuitry. Other models are more advanced, e.g considering the transfer function of the read-out electronics [5]. In this work, through mixed-mode TCAD simulations, we first analyze the behaviour of an experimental SPAD, propose an equivalent model of the transient response of the three identified mechanisms and extract the corresponding parameters. Secondly, an equivalent SPICE compact macro-model is built to embed the intrinsic response of the SPAD and validated by comparison with the full TCAD results.

II. Mixed-mode TCAD modelling

Mixed-mode TCAD *Silvaco* software [6] is used to combine a full semiconductor numerical simulation of the avalanche diode physical structure and a lumped-element model of the quenching resistor [7].

The detector we study here is an ultra-thin ultraviolet backside-illuminated SPAD with $650\,\mathrm{nm}$-thin silicon body fabricated in complementary metal-oxide-semiconductor (CMOS) using silicon-on-insulator (SOI) technology, as described in [8]. Measurements have shown a low leakage current ($\approx 0.1\,\mathrm{pA}$), a low breakdown voltage of $8.5\,\mathrm{V}$ and a peak quantum efficiency (QE) of 96.41% under a wavelength of $423\,\mathrm{nm}$ at $4\,\mathrm{V}$ excess voltage.

A. SPAD pixel structure

The pixel layout (Fig. 1a) is composed of a SPAD in series with an integrated quenching resistor, with a pixel size of $55\,\mu\mathrm{m}$ x $75\,\mu\mathrm{m}$. The 2D TCAD simulated diode structure is shown in Fig. 1b. The buried oxide (BOX) is $1\,\mu\mathrm{m}$ thick and the upper oxide layer is $200\,\mathrm{nm}$ thick. The anode-cathode pitch distance is $20\,\mu\mathrm{m}$ and the equivalent width is $35\,\mu\mathrm{m}$ according to the perimeter of the 3D actual diode (Fig. 1a). The quenching resistor is connected at the cathode of the SPAD to control the avalanche, as presented in Fig. 1c. It is simulated using lumped elements with a resistance R_q (usually a few hundred kiloohms) and a parasitic capacitance C_q (few femtofarads) [10]. In this work, R_q is equal to $440\,\mathrm{k}\Omega$ whereas C_q is set to $6\,\mathrm{fF}$ according to our design and measurements.

B. Simulations

An equivalent model (Fig. 1d) represents the first-order transient response of the SPAD when reverse-biased above the breakdown voltage V_{bd}. When the diode is quiescent, the switch is open and the model is only characterised by its junction capacitance C_d. When the avalanche is triggered, the switch is closed and the generated current is given by the voltage drop across the internal resistance R_d due to V_{bd}.

1) The resistance R_d and the breakdown voltage V_{bd} are firstly estimated by least-square linear approximation of the breakdown simulated dark DC I-V curve (not shown here) [5],

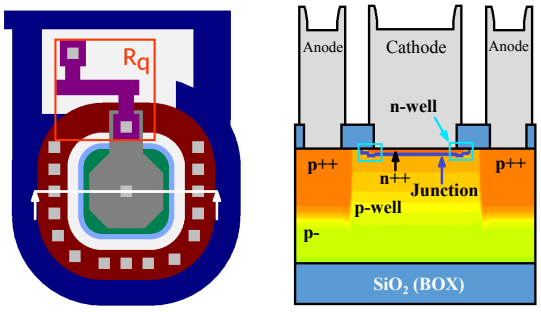

(a) Pixel layout

(b) SPAD 2D cross-section

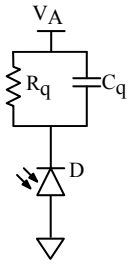

(c) Quenching pixel

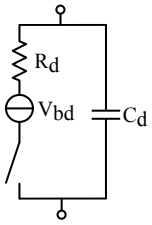

(d) SPAD equivalent model

Fig. 1. (a) Pixel layout inspired from [8]. The red square locates the integrated quenching resistor. The cross-section line shows the section used for the 2D TCAD simulation. (b) Physical 2D cross-section of the SPAD in TCAD, adapted from [8]. (c) $R_q - C_q$ lumped-element model of the quenching resistor connected at the cathode of the SPAD. (d) Equivalent model of the SPAD.

leading to $142\,\Omega$ and $7.7\,\mathrm{V}$, respectively. The structure has a lower breakdown voltage compared to the $8.5\,\mathrm{V}$ previously studied [8], due to process modifications.

2) The main contribution of the junction capacitance C_d is the depletion capacitance through the PN junction, which depends on the bias voltage. The capacitance obtained by small-signal TCAD AC simulation just before breakdown is shown in Fig. 2. At low and moderate frequencies, the capacitance is independent of the frequency. At higher frequencies, the minority carriers cannot respond to the rapidly varying voltage across the device due to their finite mobility and recombination lifetime. As a result, the device capacitance drops to a low value. The frequency at which the capacitance drops is associated with the cut-off frequency of the diode in the GHz range [9].

3) For the transient simulation, the diode is reverse-biased above breakdown voltage, at a value of $V_A = V_{bd} + V_{ex}$, where the excess voltage V_{ex} is set around $3\,\mathrm{V}$ [8]. A first quasi-static simulation is performed to reach this bias point without triggering the diode [10]. The Shockley-Read-Hall (SRH) recombination is neglected to only consider the avalanche triggered by photons. Next, Fig. 3 describes the transient response of the SPAD after a $1\,\mathrm{ns}$ light pulse at $480\,\mathrm{nm}$ wavelength with a power of $1 \times 10^{-4}\,\mathrm{W/cm^2}$. The light triggers the avalanche mechanism, which generates a high current peak up to $1.95\,\mathrm{mA}$. It induces a voltage drop across the quenching resistor and lowers the cathode voltage down to the breakdown voltage, stopping the process. The breakdown voltage retrieved from the transient simulation is

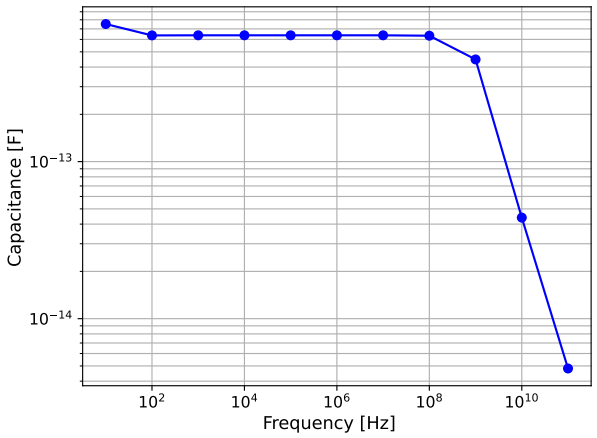

Fig. 2. Junction capacitance of the SPAD C_d regarding the frequency extracted using mixed-mode simulation. The value is taken at a bias voltage just before the breakdown.

about $6.344\,\mathrm{V}$, which is lower than that of the dark DC I-V curve. This difference can be attributed to the non-equilibrium increase in carrier concentration due to the avalanche triggered by light. At this bias, the self-sustaining current is about $7\,\mu\mathrm{A}$ (Fig. 3, left). Then, the residual current slowly recharges the cathode node through the quenching resistor up to its initial bias voltage (Fig. 3, right).

The two slopes shown in Fig. 3 (left) can be explained by drift and diffusion mechanisms [9]. As outlined in Fig. 4 (left), the carriers located in the depletion region are rapidly extracted, while a second contribution based on the diffusion of the carriers outside the depletion region causes a delayed current pulse. A similar TCAD simulated response has already been reported in [10], in the case of quenching at the anode, with a current peak in the mA range and double slopes in the quenching phase.

III. SPICE COMPACT MODELLING

The SPICE macro-model we propose (Fig. 5) is composed of three equivalent diode sub-circuits. Each one is modelled by the equivalent circuit shown in Fig. 1d. The switch is closed by a signal in the ps-range to simulate a photon trigger. Compared to the conventional approach, the switch is here modelled in SPICE by a voltage-controlled resistance, to obtain a physical rise of the current. When off, the resistance is considered as an open circuit. When on, it decreases exponentially to simulate the fast rise of the avalanche process.

Each equivalent diode sub-circuit describes a different physical mechanism that occurs after the light excitation. Because these mechanisms arise at different timescales and speeds, the junction capacitance will take a different value, as can be inferred from Fig. 2. These values are obtained by extracting the time constants τ from the transient TCAD simulation (Fig. 3) through the slope of the log-scale current taken at half of the current dynamic range of each region. The capacitances are retrieved through the following relation:

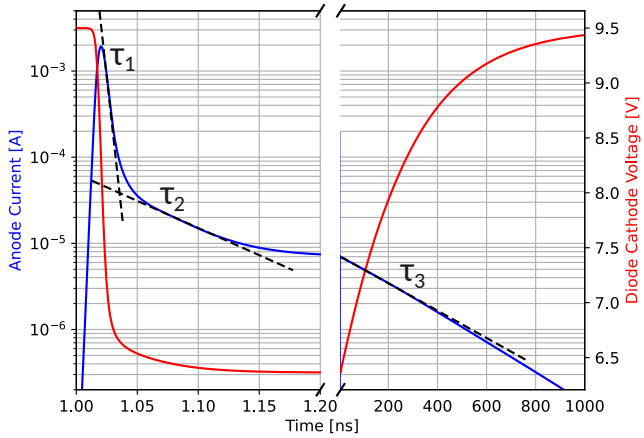

Fig. 3. Transient response of the SPAD to a light pulse sent after 1 ns. The anode current is represented in blue (left axis) and the cathode voltage in red (right axis). The left part of the graph is a 200 ps-long zoom on the fast response induced by the light excitation. The black lines describe the different slopes linked to the time constants of the drift (τ_1) and diffusion (τ_2) currents. The right part of the graph shows the slow recharge (τ_3) of the avalanche diode by the quenching resistor.

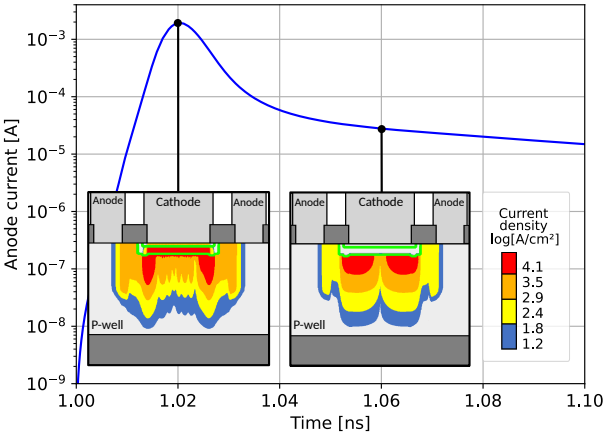

Fig. 4. Temporal evolution of the current density in the TCAD simulated layout after a light pulse excitation. The depletion region is delimited by a green line. At 1.02 ns, the carriers in the depletion region are rapidly swept out due to the high electrical field (left inset) while diffusion carriers from the quasi-neutral region take a longer time to be extracted (right inset).

$$\tau = C_{eq} R_{eq}, \tag{1}$$

with the equivalent capacitance $C_{eq} = (C_q + C_d)$ and the equivalent resistance $R_{eq} = (R_q || R_d)$.

The first diode sub-circuit (Fig. 5a) models the main photo-response current. The switch is closed by a ramp signal V_{ramp} to start the avalanche process induced by the light. When closed, the equivalent circuit generates a high current pulse and the cathode voltage V_{K1} drops abruptly. After the pulse, the command signal V_{ramp} is kept high to induce the self-sustaining current of 7 µA, generated through the voltage drop across R_q. Given a time constant of about 3.7 ps for the fast pulse related to drift, the equivalent capacitance is about 18.7 fF. This corresponds to a depletion capacitance Cd_1 of about 12.7 fF, as observed at very high frequency in Fig. 2.

The second diode sub-circuit (Fig. 5b) simulates the diffusion process of the carriers generated outside the depletion region. Since slower, its contribution is delayed compared to the first pulse. Hence, the second switch is closed after a delay $T_{delayed}$ of 25 ps estimated from Fig.3, through the signal $V_{delayed}$. The diffusion process has a time constant τ_2 of about 42 ps after removing the contribution of the current flowing through R_q. It yields an estimated junction capacitance C_{d2} of about 289 fF. Since this current contribution is delayed, the voltage seen at the cathode has already dropped. This is considered by applying a bias voltage V'_A set as: $V'_A = V_{K1}(t = T_{delayed}) = 6.7\,\text{V}$. The sum of the currents set by the two equivalent sub-circuits expresses the total generated pulse.

The third diode sub-circuit (Fig. 5c) focuses only on recharge. The switch is closed to produce the drop of voltage from the initial bias to the breakdown voltage. After 1 ns, the switch is opened to represent the stop of the avalanche process by the quenching resistor. Since the diode is switched off, the mechanism responsible for the recharge operates at a lower frequency, which results in a high capacitance C_{d3} (Fig. 2). The associated time constant τ_3 is about 277 ns in the simulated transient recharge. When off, the diode equivalent resistance is very large compared to R_q, which gives an equivalent capacitance of about 0.63 pF. It corresponds to the low-frequency value of C_d in Fig. 2.

In a last step, the above estimated sub-model parameters have been adjusted to fit the full SPICE simulation on the transient response of the TCAD simulation, yielding the final SPICE parameters given Tab. I.

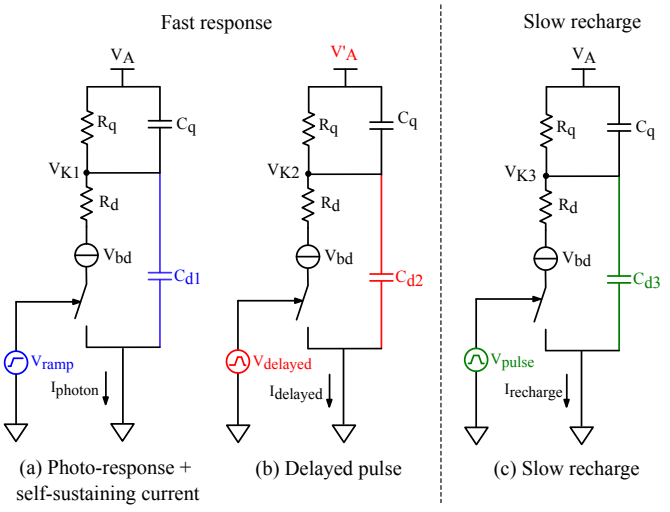

Fig. 5. Proposed SPICE two-phase macro-model of the SPAD composed of three equivalent diode sub-circuits. It describes the fast photo-response pulse, through (a) a first photo-pulse and (b) a delayed diffusion current. It also models (c) the slow recharge of the diode after the quenching. V_{ramp} and V_{pulse} rise at $t = 0$ while the $V_{delayed}$ rises at $t = T_{delayed}$.

TABLE I
SUMMARY OF SPICE MODEL PARAMETERS.

V_A [V]	V'_A [V]	V_{bd} [V]	R_q [kΩ]	C_q [fF]
9.5	6.7	6.344	440	6
R_d [Ω]	C_{d1} [fF]	C_{d2} [fF]	C_{d3} [pF]	
142	22	250	0.6	

Fig. 6 presents the response of the SPICE model compared to the TCAD simulation. In the first phase (Fig. 5, left), it describes the physical current rise induced by the light-triggered avalanche mechanism and correctly reproduces the different current contributions. A first pulse of 1.97 mA arises 20 ps after the light excitation. The pulse is followed by a delayed response after 25 ps and a self-sustaining current of 8.5 µA. It accurately represents the TCAD simulated current peak (1.95 mA) but slightly overestimates the self-sustaining current (7 µA). The cathode voltage drops from its initial bias voltage of 9.5 V to the non-equilibrium breakdown voltage of 6.344 V. The first part of the drop (down to 6.7 V) is dominated by the fast pulse while the second part is given by the delayed response. In the second phase (Fig. 5, right), the model shows the slow 1 µs-recharge of the cathode done through the quenching resistor.

Literature-based models usually extract model parameter values from measurement, where the parasitic capacitance or limited read-out bandwidth tends to smooth out the internal signal. By relying on TCAD simulations, our model allows for the extraction of intrinsic values, thereby revealing the distinct mechanisms that occur during the current-voltage transient response. As a result, this model provides a more accurate representation of the physics behind the current generation.

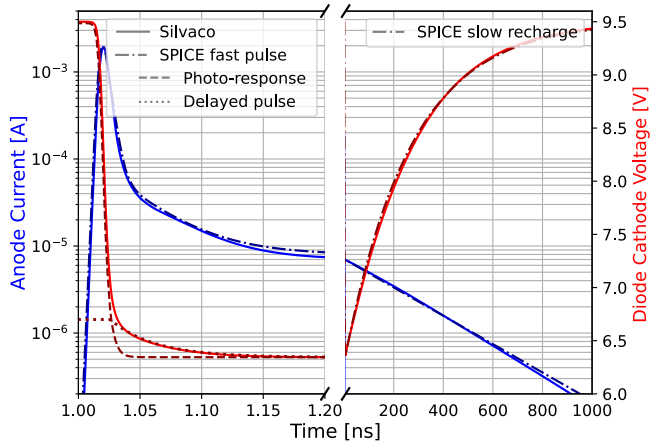

Fig. 6. SPICE Transient response of the proposed model vs. the TCAD mixed-mode simulation. On the left part of the graph, the red dashed line is the voltage drop induced by the first current pulse, while the dotted line is the voltage drop due to the delayed pulse. The blue dot-dashed line is the sum of the currents induced by the two first equivalent diode sub-circuits.

IV. CONCLUSION

This paper describes a method to accurately represent the intrinsic transient response of a TCAD-simulated SPAD with a compact SPICE model. The developed two-phase macro-model describes the fast double-response to a photon excitation and the slow recharge induced by the quenching resistor. This is achieved by using three parallel compact equivalent sub-circuits of the diode, each characterising a different physical mechanism. Their associated junction capacitance is linked to the physical time constant of each phenomenon. The first diode sub-circuit, describing a fast pulse reaching about 2 mA, has a capacitance in the tens of femtofarad and a time constant of about 3 ps, corresponding to a drift process with a very high-frequency depletion capacitance. The second diode sub-circuit, representing a slower diffusion current induced after the fast pulse, has a capacitance in the hundreds of femtofarad and a time constant of 35 ps leading to a self-sustaining current of about 8.5 µA. The third diode sub-circuit, modelling the slow recharge, has a capacitance of about tenths of a picofarad linked to the low-frequency diode depletion capacitance and a time constant of 264 ns.

Compared to classical models that rely on measurements, TCAD simulations enable the extraction of intrinsic values, providing a more accurate representation of the physics behind the current-voltage full transient response. This SPICE model can be used to design a dedicated integrated (at pixel level) read-out circuit with active recharge by accurately reproducing the current and voltage induced by the SPAD and the quenching resistor after a photon excitation.

REFERENCES

[1] D. Bronzi, F. Villa, S. Tisa, A. Tosi, and F. Zappa, "SPAD Figures of Merit for Photon-Counting, Photon-Timing, and Imaging Applications: A Review," IEEE Sensors J., vol. 16, no. 1, pp. 3–12, Jan. 2016, doi: 10.1109/JSEN.2015.2483565.

[2] S. Tisa, F. Zappa, A. Tosi, and S. Cova, "Electronics for single photon avalanche diode arrays," Sensors and Actuators A-physical - SENSOR ACTUATOR A-PHYS, vol. 140, pp. 113–122, Oct. 2007, doi: 10.1016/j.sna.2007.06.022.

[3] F. Zappa, A. Tosi, A. D. Mora, and S. Tisa, "SPICE modeling of single photon avalanche diodes," Sensors and Actuators A: Physical, vol. 153, no. 2, pp. 197–204, Aug. 2009, doi: 10.1016/j.sna.2009.05.007.

[4] A. Arbat, A. Dièguez, D. Gascon, J. Trenado, and Ll. Garrido, "Avalanche photodiodes for high energy particle tracking in 130 nm CMOS technology," in 2009 16th IEEE International Conference on Electronics, Circuits and Systems - (ICECS 2009), Dec. 2009, pp. 579–582. doi: 10.1109/ICECS.2009.5410849.

[5] D. Marano, G. Bonanno, S. Garozzo, A. Grillo, and G. Romeo, "A New Simple and Effective Procedure for SiPM Electrical Parameter Extraction," IEEE Sensors J., vol. 16, no. 10, pp. 3620–3626, May 2016, doi: 10.1109/JSEN.2016.2530848.

[6] *Atlas User's Manual: Device Simulation Software.* Silvaco Inc., Santa Clara, CA, 2015.

[7] H.-J. Yang and X.-L. Jin, "Device and mixed-mode simulations of single photon avalanche diode," in 2016 13th IEEE International Conference on Solid-State and Integrated Circuit Technology (ICSICT), Oct. 2016, pp. 444–446. doi: 10.1109/ICSICT.2016.7998946.

[8] I. Sabri Alirezaei, N. Andre, A. Sedki, P. Gerard, and M. D. Flandre, "An Ultra-Thin Ultraviolet Enhanced Backside-Illuminated Single-Photon Avalanche Diode With 650 nm-Thin Silicon Body Based on SOI Technology," IEEE J. Select. Topics Quantum Electron., vol. 28, no. 2: Optical Detectors, pp. 1–10, Mar. 2022, doi: 10.1109/JSTQE.2021.3129274.

[9] A. Afzalian and D. Flandre, "Physical Modeling and Design of Thin-Film SOI Lateral PIN Photodiodes," IEEE Trans. Electron Devices, vol. 52, no. 6, pp. 1116–1122, Jun. 2005, doi: 10.1109/TED.2005.848080.

[10] D. Issartel et al., "Architecture optimization of SPAD integrated in 28 nm FD-SOI CMOS technology to reduce the DCR," Solid-State Electronics, vol. 191, p. 108297, May 2022, doi: 10.1016/j.sse.2022.108297.